

## Article

# Non-Invasive Investigation of a 16th-Century Illuminated Scroll: Pigments, Fillers, and Metal-Based Decorations

Lucilla Pronti <sup>1,\*</sup>, Martina Romani <sup>1</sup>, Luca Lanteri <sup>2</sup>, Francesco Bizzarri <sup>2</sup>, Claudia Colantonio <sup>3</sup>,  
Claudia Pelosi <sup>2</sup>, Chiara Ruberto <sup>4,5</sup>, Lisa Castelli <sup>5</sup>, Anna Mazzinghi <sup>4,5</sup>, Valeria Spizzichino <sup>6</sup>  
and Mariangela Cestelli Guidi <sup>1</sup>

- <sup>1</sup> INFN-Frascati National Laboratory, Via E. Fermi 54, 00044 Frascati, Italy; martina.romani@lnf.infn.it (M.R.); mariangela.cestelliguidi@lnf.infn.it (M.C.G.)
- <sup>2</sup> Department of Economics, Engineering, Society and Business Organization, University of Tuscia, Largo dell'Università, 01100 Viterbo, Italy; llanteri@unitus.it (L.L.); bizfrancesco@libero.it (F.B.); pelosi@unitus.it (C.P.)
- <sup>3</sup> Department of Science of Antiquities, University of Rome "Sapienza", Piazzale Aldo Moro 5, 00185 Roma, Italy; c.colantonio@uniroma1.it
- <sup>4</sup> Department of Physics and Astronomy, Florence University, Via G. Sansone 1, 50019 Sesto Fiorentino, Italy; chiara.ruberto@unifi.it (C.R.); anna.mazzinghi@unifi.it (A.M.)
- <sup>5</sup> INFN-Sezione di Firenze, Via G. Sansone 1, 50019 Sesto Fiorentino, Italy; lisa.castelli@fi.infn.it
- <sup>6</sup> ENEA Fusion and Technology for Nuclear Safety and Security Department, Physical Technologies for Security and Health Division, Via E. Fermi 45, 00044 Frascati, Italy; valeria.spizzichino@enea.it
- \* Correspondence: lucilla.pronti@lnf.infn.it

## Abstract

The study and preservation of illuminated manuscripts, particularly miniatures on parchment, are crucial for understanding the artistic, cultural, and technological history of the past. This research investigates the materials used in a 16th-century illuminated scroll, analyzing both the miniatures and the written text through non-invasive techniques. A multi-analytical approach was applied, including optical microscopy, Hypercolorimetric Multispectral Imaging (HMI), infrared reflectography in the 950–1700 nm range, Fiber Optics Reflectance Spectroscopy (FORS), macro X-ray fluorescence (MA-XRF) spectroscopy, Raman spectroscopy, and External Reflection Fourier Transform Infrared (ER-FTIR) spectroscopy. These methods provided a comprehensive characterization of the painting materials' chemical composition and the artistic techniques utilized, revealing new information on Renaissance materials and practices. The detected mineral pigments primarily include smalt, vermilion, lead white, and minium, which are consistent with materials commonly found in illuminated manuscripts. Aluminosilicate and calcite were identified as fillers or substrates utilized for organic dyes, particularly those generating pink hues. An uncommon finding was the green pigment, which was identified as copper hydroxynitrate. Furthermore, gold and silver were extensively employed in the decorative elements, both as metal foils and in shell pigment form. Finally, the capital letters were executed using smalt and vermilion, while the black text ink was characterized as iron gall ink, a composition typically employed on parchment supports.

**Keywords:** macro X-ray fluorescence (MA-XRF); multispectral imaging; Raman spectroscopy; External Reflection FTIR (ER-FTIR) spectroscopy; Fiber Optics Reflectance Spectroscopy (FORS); illuminated manuscript



Academic Editor: Santiago Pozo-Antonio

Received: 26 September 2025  
Revised: 15 November 2025  
Accepted: 19 November 2025  
Published: 26 November 2025

**Citation:** Pronti, L.; Romani, M.; Lanteri, L.; Bizzarri, F.; Colantonio, C.; Pelosi, C.; Ruberto, C.; Castelli, L.; Mazzinghi, A.; Spizzichino, V.; et al. Non-Invasive Investigation of a 16th-Century Illuminated Scroll: Pigments, Fillers, and Metal-Based Decorations. *Minerals* **2025**, *15*, 1252. <https://doi.org/10.3390/min15121252>

**Copyright:** © 2025 by the authors. Licensee MDPI, Basel, Switzerland. This article is an open access article distributed under the terms and conditions of the Creative Commons Attribution (CC BY) license (<https://creativecommons.org/licenses/by/4.0/>).

## 1. Introduction

Analyzing the materials in Renaissance miniatures is essential to understand the techniques, cultural context, and historical value of these artworks [1,2]. Renaissance illuminated manuscripts were created using sophisticated techniques and sometimes rare and precious materials that showcase the skill and creativity of the painters. These miniatures not only served religious, educational, and decorative purposes but also symbolized wealth and power, due to the precious materials often involved. Indeed, one key reason for analyzing materials in Renaissance miniatures is to better understand their economic and symbolic value. For example, pigments such as ultramarine blue, derived from lapis lazuli, were rare and costly, often reserved for high-status commissions [3]. Another significant aspect is understanding the chemical composition and degradation behavior of pigments, dyes, and binders [4–9]. Renaissance miniatures, like all historical artifacts, are vulnerable to environmental factors such as light, humidity, and temperature fluctuations. Inks, organic pigments, and binders can be particularly sensitive, leading to fading or discoloration over time [10–13]; preventive non-invasive investigations can provide insights on how to improve proactive conservation actions [14–16].

An effective approach for analyzing Renaissance miniatures involves the use of non-invasive and non-destructive multispectral and hyperspectral imaging techniques to detect inhomogeneities in the spectral behavior of the materials and to uncover hidden details [5,17–19]. Infrared reflectography (IRR), for example, is a valuable tool in revealing preliminary sketches and changes made during the artistic process that are not visible to the naked eye [20–24]. This technique helps scholars and conservators understand the evolution of the artwork, offering a glimpse into the artist's planning and modifications.

Spectroscopic analyses are essential for identifying specific pigments, dyes, binders, and supports used in the creation of miniatures. Among the most commonly employed methods are X-ray fluorescence (XRF), Raman spectroscopy, and Fiber Optic Reflectance Spectroscopy (FORS) [1,4,6,13,25–30]. These techniques allow for the detection of elemental and molecular components within the pigments and materials, helping to identify the exact substances used in the artwork. Moreover, Fourier Transform Infrared spectroscopy (FTIR) also plays an important role, providing in-depth compositional information about the pigments and binders used in the miniature without causing damage [31]. These analyses contribute to the reconstruction of the artist's methods and offer valuable insights into the technical knowledge and creativity that shaped the piece. Moreover, these methods are crucial in assessing the stability of the miniature and recommending appropriate conservation strategies. For example, the identification of light-sensitive pigments may inform best practices for the manuscript's display and storage, helping to prevent further deterioration.

In this study, we present the analyses conducted on a 16th-century illuminated manuscript during a Training Camp organized in 2021 by INFN, ENEA, and the University of Tuscia, in the field of the Center of Excellence DTC-Lazio.

This specific artifact, precisely dated to 1585 AD, is an important historical document from the Counter-Reformation period, recording the official approval by Frater Sixstus Fabri Lucensis, Master General of the Dominican Order, for the newly established Brotherhood of the Corpus Christi of Civitella d'Agliano to build an altar and a chapel. Given the artifact's historical importance and precise dating, a scientific investigation into its materials (pigments, binders, and precious metals) was undertaken. This research serves both to corroborate the document's historical value and to increase the understanding of the execution techniques of manuscripts from this specific period and geographical area.

Therefore, the focus of this study is to achieve a comprehensive understanding of the used pigments, fillers, and metal-based materials through a multi-analytical, non-invasive

approach that combines imaging techniques with spectroscopic analyses, including scanning mode investigations. Hypercolorimetric Multispectral Imaging (HMI) [32–36] allowed us to acquire data across a wide spectral range, from ultraviolet (UV, 300 nm) to near-infrared (NIR, 1000 nm), enabling us to perform various digital processing techniques on the calibrated images. To investigate the underdrawings more thoroughly, IR-reflectography images were captured in the 950–1700 nm range. Spectroscopic techniques such as macro X-ray fluorescence (MA-XRF), Raman Spectroscopy, Fiber Optic Reflectance Spectroscopy (FORS), and External Reflection Fourier Transform Infrared spectroscopy (ER-FTIR) were employed for a detailed analysis of the pigments, binders, and supports. Finally, optical microscope observation was employed to identify specific details of the pictorial techniques, particularly regarding pigment mixtures.

## 2. Materials and Methods

### 2.1. The Illuminated Parchment

The illuminated parchment, shown in Figure 1, is dated to 1585 AD (as reported on the document itself) and is now preserved in the parish Church of the Saints Valentine and Hillary in Viterbo (Italy). Originally, the scroll belonged to the Brotherhood of the Corpus Christi of Civitella d’Agliaio, a small town in the province of Viterbo, part of the Diocese of Bagnoregio at the time of the creation of the text. The information about the parchment was derived exclusively from the text written on it in the Latin language, as usual for ecclesiastical and civil documents in that period. No written sources and archival references were found concerning the parchment, so translation and interpretation were fundamental for understanding its significance and value. The main concepts expressed in the parchment text are summarized as follows:

- The parchment is an important document from the Counter-Reformation period, where the strength of the orthodoxy of the Catholic Church expressed by the Dominican Order is highlighted, starting from the title (*Sit Nomine Domini Benedictum in Saecula Amen; Be the Name of God Blessed Forever Amen*).
- The text indirectly reflects the apprehension and insistence of the members of a small and recently established Brotherhood, the Corpus Christi of Civitella di Agliaio, who requested approval from the Dominicans. In fact, the members of the Brotherhood were worried about not having acted according to the expected rules, i.e., by asking permission from the Dominicans.
- The document, in response to the requests of the Brotherhood, is drawn up by Frater Sixtus Fabri Lucensis, Generalis Magister of the Dominican Order and Professor of Theology. He confirmed the approval and guaranteed the authorization to constitute the Brotherhood through *patentibus literis* (the parchment itself) to build an altar and a chapel in the Church of San Pietro in Civitella d’Agliaio in the Diocese of Bagnoregio.

The illuminated frame is characterized by decorative elements and by four saints represented in the upper part (left and right sides) and in the central part (left and right sides). The two saints in the central parts are clearly Dominican friars, easily recognizable by their typical white dress with black mantle. The Dominican on the left side is Saint Peter of Verona identified by the saber on his head, with which he was killed. The other Dominican on the right side is Saint Thomas from Aquino, whose iconographic symbols are the ostensory, the book, and the sun in his chest.

The saints in the upper part of the frame are St. Peter (identified by the key) and St. Paul, who can be identified by the sword and from his usual association with St. Peter. The Christ Child is painted in the middle circle in a blue background with golden stars.

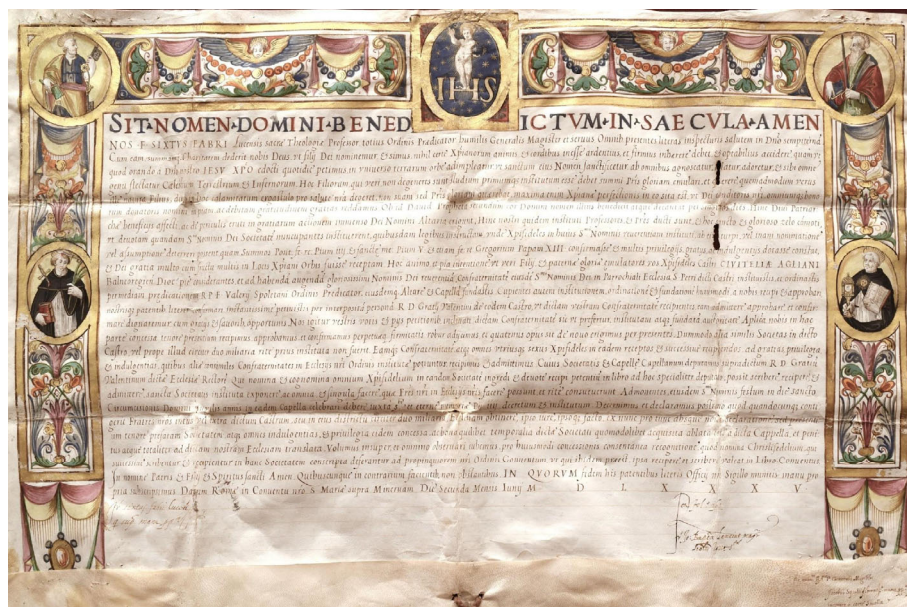


**Figure 1.** The illuminated scroll.

## 2.2. Experimental Section

### 2.2.1. Hypercolorimetric Multispectral Imaging (HMI)

The initial phase of the diagnostic campaign on the artwork involved a multispectral imaging investigation within the UV-Vis-NIR spectral range. This technique provided a comprehensive overview of the artwork across various regions of the electromagnetic spectrum, aiding in the identification of anomalies, past restorations, and areas exhibiting similar spectral features.

Multispectral imaging was performed with the HMI system developed by Profilocolore (Rome, Italy) in 2013 based on the following main components:

- (i) The acquisition device is made up of a Nikon D800 camera (Nital SpA, Moncalieri Torino, Italy) modified in full range to register images in the spectral range 300–1000 nm and is equipped with a 60 mm lens; optical filters for UV-Vis and Vis-IR acquisition (named filter A and filter B, respectively), for UVF (U V-IR cut filter coupled with filter A), and light sources consisting of two modified NEEWER (Neewer, Shenzhen, China) 750II Flashes Speedlite TTL flashes with LCD display and wireless triggers. The flashes were modified by removing their front plastic lenses, thus allowing emissions in the 300–1000 nm region for multispectral imaging, and two UV CR230B-HP 10W LED projectors (peak emission at 365 nm, for ultraviolet fluorescence) (Madatec srl, Pessano con Bornago, Milano, Italy) were used; white references patches positioned around the parchment, along with a ColorChecker (version 8.0) made of 36 standard colors and 8 grayscale patches, plus two reference white and two blacks; the illuminating sources were positioned at about 45° with respect to the artwork surface;
- (ii) The calibration software, named SpectraPick® (Version 1.2, created by Profilocolore, Rome, Italy) allows obtaining imaging data for seven monochromatic bands (.tiff images) centered at 350, 450, 550, 650, 750, 850, and 950 nm and the visible RGB output;
- (iii) The processing software, named PickViewer® (Version 1.2, created by Profilocolore, Rome, Italy) enables the extraction of information to support materials characterization and to highlight surface details by applying digital image processing tools to the calibrated bands.

The processing software was used to gather the infrared false color (IRFC) and ultraviolet false color (UVFC) images, by applying the specific algorithm for false color output production. Moreover, it was used to obtain chromatic similarity maps through the specific algorithm. This enables the calculation of the chromatic values of a selected area of some pixels (in our case  $3 \times 3$  pixels) in the 300–1000 nm range and the use of these values as a filter to enhance all the pixels in the image with a similar (within a selected confidence threshold) chromatic response. The process allows for the evaluation that materials with a similar chromatic signature have similar chemical–physical features or composition. The software PickViewer works by selecting an area in the RGB image and then compares the chromatic values of that area with those of the whole image. The result is displayed as a black/white image where the white pixels have high similarity to each other, and the black ones have no similarity.

#### 2.2.2. Infrared Reflectography in the 950–1700 nm Spectral Range (IRR)

Infrared reflectography (IRR) allows us to identify the underdrawings and/or *pentimenti* depending on the pictorial layer's transparency in the infrared range. The infrared reflectography in the 950–1700 nm range was performed with a SWIR camera (Hamamatsu "C12741-03", Hamamatsu Photonics, Shizuoka, Japan), which has an InGaAs sensor with the spectral range at 950–1700 nm, a resolution of  $640 \times 512$ , and a pixel pitch of  $20 \mu\text{m}^2$ . The digital output is 14-bit. For illumination, two halogen lamps (300 W) were placed at  $45^\circ$  with respect to the analyzed parchment.

#### 2.2.3. MA-XRF

Macro X-ray fluorescence (MA-XRF) allowed the elemental characterization of the inorganic materials in the parchment, providing the elemental distribution maps of the analyzed areas.

A portable XRF scanner developed by the INFN-CHNet network at LABEC Laboratory (INFN-Fi, Sesto Fiorentino, Italy) for cultural heritage applications was employed [37]; this instrument is compact, lightweight, and provided with a dynamic positioning system, allowing the analysis of non-planar surfaces. A helium flow control system to enhance the detection of low energy X-rays is also available when needed.

The measuring head consists of a Mo-anode X-ray tube (Moxtek, Orem, UT, USA, 40 kV maximum voltage, 0.1 mA maximum anode current), an SDD detector (Amptek XR-100 SDD with OEM configuration, Amptek, Bedford, MA, USA), and a telemeter to measure the sample-to-head distance.

The low radiation emission of the X-ray tube (40 kV maximum voltage and 0.1 mA maximum anode current) allows in situ measurements also in museums and with the public, as in this case.

Homemade software controls all the scanning process, from the motion along the three positioning stages (Physik Instrumente, Karlsruhe, Germany, 300 mm travel range in X-, 300 mm Y- and 50 mm in Z-direction) to the data acquisition and the data processing to reconstruct the elemental distribution maps. These are obtained by selecting a region of interest (ROI) in the acquired XRF spectrum, usually corresponding to the characteristic X-ray line of an element, and assigning to each pixel a grayscale level corresponding to the X-ray counts falling within the ROI: white is assigned to the maximum value, while black is assigned to the minimum. Thus, the same gray tone in elemental maps obtained from different ROI of the same spectrum may correspond to different counts, and different gray tones may correspond to the same number of counts.

The experimental conditions for this campaign were as follows:

- For the illuminated parts: 38 kV anode voltage, 70  $\mu\text{A}$  filament current, 10 mm/s scanning velocity, and 0.5 mm step in both X and Y directions. Beam diameter on the sample surface  $\sim 1$  mm, no He flow.
- For the written part: 30 kV anode voltage, 95  $\mu\text{A}$  filament current, 0.5 mm/s scanning velocity, and 0.25 mm step in both X and Y directions. Collimator diameter 0.4 mm, no He flow.

#### 2.2.4. Raman Spectroscopy

Raman spectroscopy measurements were performed to identify the molecular composition of pigments and dyes employed by the painter or related to previous restoration treatments. It was performed in situ using a portable BWTek (B&W Tek, Plainsboro, NJ, USA) i-Raman system equipped with a probe with a spot on the target of about 3 mm. The system is equipped with a 785 nm laser source and a cooled 2048-pixel CCD array detector, with a spectral resolution of  $3\text{ cm}^{-1}$  and coverage of the spectral range from 0 to  $4000\text{ cm}^{-1}$ . Its maximum power is 30 mW. The instrument is calibrated in Raman shift by the manufacturer, which periodically carries out system maintenance. At the beginning of each measurement campaign, the spectral calibration is checked using a reference sample in polytetrafluoroethylene (PTFE), characterized by clean and well-defined Raman bands. For the present campaign, the laser power was kept between 1 and 20% of the maximum rated power, with an integration time of 10–30 s.

#### 2.2.5. External Reflectance FT-IR (ER-FTIR) Spectroscopy

FT-IR measurements were applied to complement the Raman spectroscopy ones to identify the support and the pigments. FT-IR measurements were performed using a portable IR spectrometer ALPHA-II (Bruker Optics, Ettlingen, Germany) equipped with a DTGS detector, owned by DAFNE-Light (INFN-LNF, Frascati, Italy). The measurements were collected in reflection mode over the  $7000 - 360\text{ cm}^{-1}$  spectral range, with a resolution of  $4\text{ cm}^{-1}$  and using 128 scans. Three spectra of each investigated area were measured to generate an average spectrum. The acquired spectra were represented as Pseudo-absorbance spectra [ $\log(1/R)$ ;  $R = \text{reflectance}$ ]. In reflection mode, absorption bands can be distorted due to surface and volume reflections. Surface reflection may cause distortion in the band shape, resulting in derivative-like features and inversion bands (Reststrahlen effect). On the other hand, volume reflection (also known as diffuse reflection) produces bands similar to those obtained in transmission mode [38,39]. In this study, derivative-like shapes are denoted by “\*” and inversion bands by “+”.

#### 2.2.6. Optical Microscopy

Optical microscopic observations were performed with two devices in order to visualize the painted surface morphologies. The  $20\times$  magnifications were obtained using a Nikon D750 reflex camera equipped with a microscope objective, while lower magnifications were achieved with a Dino-Lite equipped with white LED and UV light (AnMo Electronics Corporation, Hsinchu City, Taiwan). By exciting the painting materials using a UV source, it is possible to obtain UV fluorescence images.

#### 2.2.7. Fiber Optic Reflectance Spectroscopy (FORS)

The FORS measurements were performed to identify dyes. The FORS spectra were acquired using a spectrometer, an optical probe, and a halogen light source. The spectrometer (ATP2000P, Optosky, Xiamen, China) operates within a spectral range of 200–1100 nm, providing a spectral resolution of 2 nm. The optical probe directs light onto the sample

surface and collects the emitted or reflected light at a  $90^\circ$  angle, ensuring perpendicular illumination and detection. A halogen lamp (AVALIGHT-HAL-S-MINI2, Avantes, Apeldoorn, The Netherlands) was used as the excitation source. The FORS spectra were normalized against a Spectralon<sup>®</sup> Diffuse Reflectance Standard (Labsphere, North Sutton, NH, USA).

### 3. Results and Discussion

#### 3.1. Painting Technique

##### 3.1.1. The Support

The ER-FTIR measurements confirmed that the support is parchment by identifying the derivative-like bands at  $1650^*$  and  $1550^*$   $\text{cm}^{-1}$  attributable to the amide I and amide II of collagen [3]. Moreover, calcium carbonate was detected via the bands at  $2515$  [ $\nu_1 + \nu_3$  and/or  $2\nu_2 + \nu_4$  ( $\text{CO}_3^{-2}$ )],  $1787$  [ $\nu_1 + \nu_4$  ( $\text{CO}_3^{-2}$ )],  $1416^+$  [ $\nu_3$  antisymmetric stretching of  $\text{CO}_3^{-2}$ ], and  $870^*$   $\text{cm}^{-1}$  [ $\nu_2$  out-of-plane bending of  $\text{CO}_3^{-2}$ ] [39] (Figure 2), consistent with traditional practices in manuscript preparation, where calcium-based materials were commonly applied to provide a smooth, durable, and stable surface for writing and painting [2]. The presence of Ca-based compounds is also confirmed by MA-XRF analysis.

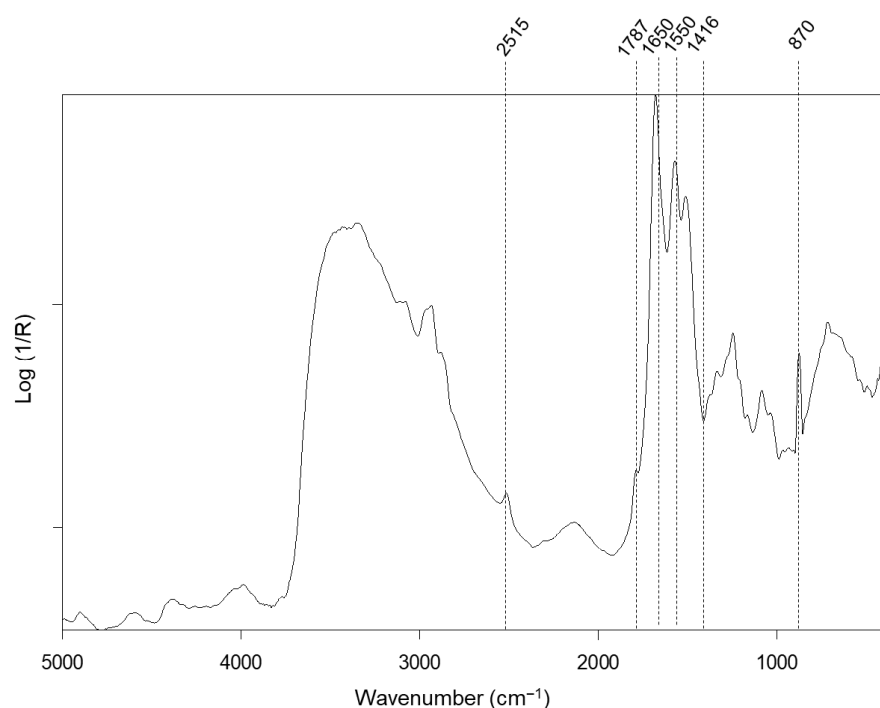


**Figure 2.** ER-FTIR spectrum of the support.

Regarding the parchment's conservation state, the RGB image, acquired through the HMI system together with the ColorChecker used as chromatic reference (Figure 3a), shows that the parchment is not perfectly flat due to the folds that probably affected the scroll in the past. In fact, the parchment is currently embedded in the frame and protected with a glass, but in the past, it was folded.

In Figure 3b, in addition to the general light blue fluorescence associated with the organic nature of the parchment, some yellow fluorescence spots (not yet characterized) are detected in the left lower side and in the central part in correspondence of a folding. Overall, from the analysis of the UVF image, it is possible to state that the parchment is in a good state of conservation, apart from the heavy signs left by the folding suffered in the past.

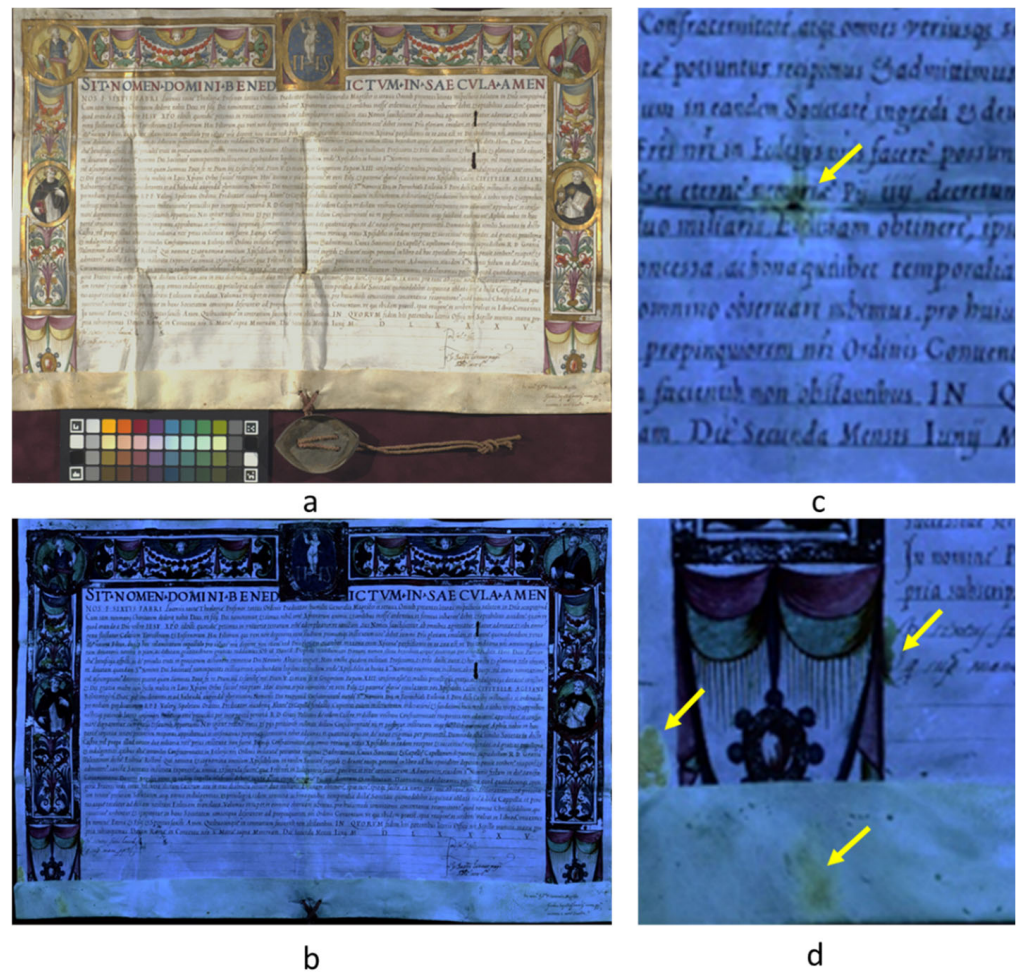


**Figure 3.** The RGB calibrated image (a) and the ultraviolet fluorescence image (b) of the parchment. Magnification of two areas of the ultraviolet fluorescence image affected by yellow spots (c,d), indicated by yellow arrows.

### 3.1.2. Underdrawings

Infrared reflectography (both achieved with the HMI system and InGaAs camera) highlights great care in the definition of the pictorial composition because the decorative elements in the foreground (i.e., books, the ostensory, etc.) were already provided in the drawing and, thus, were not directly painted on the underlying backgrounds, as shown in Figures 4 and 5. Infrared reflectography reveals the underdrawings, especially in areas painted with infrared-transparent pigments. For example, the detail of the palm clearly shows two lines beneath it, indicating the edge of the mantle (Figure 5d, highlighted with a yellow arrow). Generally, the more intense and contrasting strokes in the IRR images are also clearly visible to the naked eye, indicating they were made on top of the paint layer specifically to emphasize the features like folds, outlines, and facial details (an example is reported in Figure 5b, highlighted with red arrows). Finally, a more detailed description of the materials used will be provided in Section 3.2.



**Figure 4.** RGB images (a,c,e,g) and IRR images (b,d,f,h) of the saints taken in the range 900–1700 nm (InGaAs camera).



**Figure 5.** RGB images (a,c,e) and IRR images (b,d,f) of some details in the range 900–1700 nm (InGaAs camera). Several lines associated with the drawing are marked with yellow and red arrows.

### 3.2. Pigment Identification

To identify the pigments used, MA-XRF analysis was performed on selected areas of the illuminated scroll. Specifically, Figure 6 shows the distribution of the detected elements in three areas corresponding to the depiction of the three saints.

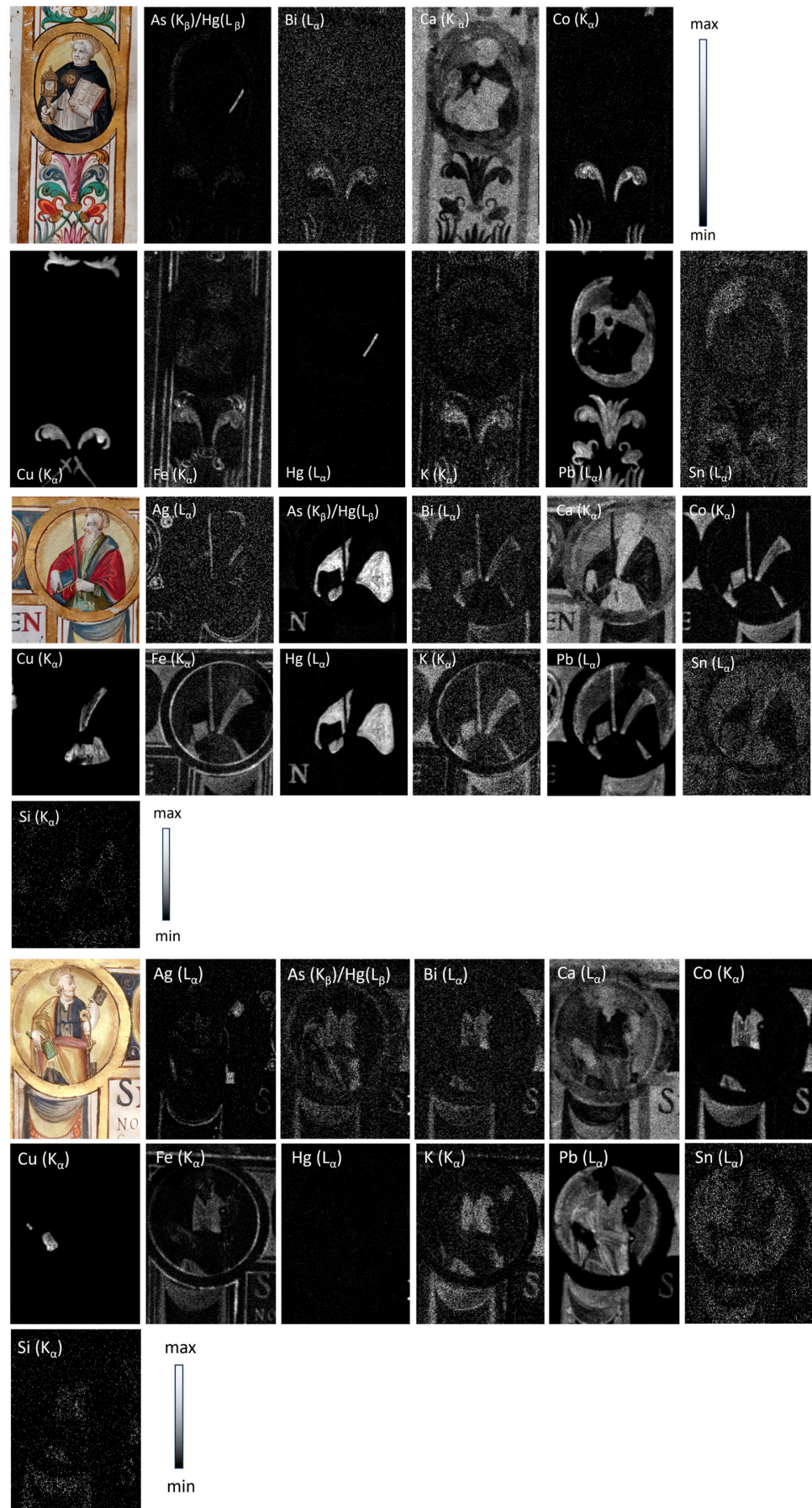
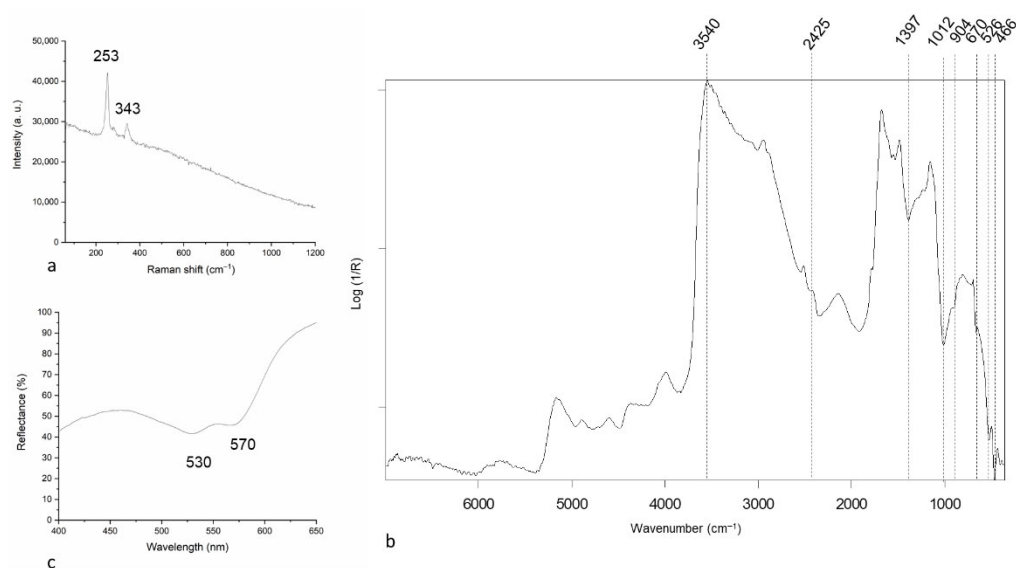


Figure 6. XRF maps corresponding to three saints.

The red hue is primarily composed of mercury (Hg), as shown in Figure 6, indicating the use of vermilion or cinnabar (HgS), confirmed by Raman spectroscopy through the characteristic peaks at 253 and 343  $\text{cm}^{-1}$  (Figure 7a) related to the Hg-S stretching mode (symmetric A1 and the transverse E mode, respectively [40]). In antiquity, cinnabar was the primary natural source of mercury sulfide (HgS). Significant deposits of this ore were historically mined and continue to be found, notably in China and Almadén, Spain [1]. Mercury sulfide could also be created artificially by carefully heating elemental mercury and elemental sulfur together. When produced in this manner, the resulting pigment was often referred to as vermilion. Both cinnabar and vermilion were widely employed as a pigment in the creation of illuminated manuscripts because their intense color and their high opacity made them ideal for decorative borders and the initial letters [41].



**Figure 7.** Raman spectrum of the red hue (a), ER-FTIR (b), and FORS (c) spectra of the pink hue.

In the pink hues, MA-XRF reveals the presence of Pb, and the ER-FTIR spectrum (Figure 7b) detects bands at 3540  $\text{cm}^{-1}$  [OH stretching modes], 2425  $\text{cm}^{-1}$  [ $\nu_1 + \nu_3$  and/or  $2\nu_2 + \nu_4$  ( $\text{CO}_3^{-2}$ )], 1397+  $\text{cm}^{-1}$  [(antisymmetric  $\text{CO}_3^{-2}$  stretching ( $\nu_3$ ))], and 670+ [ $\nu_4$  in-plane bending of  $\text{CO}_3^{-2}$ ]  $\text{cm}^{-1}$ , which are attributed to hydrocerussite [ $\text{Pb}_3(\text{OH})_2(\text{CO}_3)_2$ ] [39]. Generally, hydrocerussite was intentionally used in illuminations as a fine-quality pigment, due to its high refraction and opacity, in contrast with cerussite ( $\text{PbCO}_3$ ), which had the lowest binding power [42]. Additionally, the presence of aluminosilicates, indicated by bands at 1030–1000+  $\text{cm}^{-1}$  (Si-O-Si asymmetric stretching), 904+  $\text{cm}^{-1}$  (asymmetric stretching Si-O-Al), 526+  $\text{cm}^{-1}$  [ $\nu_s$  Si-O-Al], and 466+  $\text{cm}^{-1}$  [O-Si-O(Al) bending] [43], suggests the use of dyes, as confirmed by the FORS analysis, revealing two absorption bands at 530 and 570 nm (Figure 7c) [44].

These findings, combined with the detection of green fluorescence in the UVFC and a yellow-orange hue in the IRFC image, suggest the presence of an insect-derived lake (Figure 8) [45,46]. Lakes, or lake pigments, were historically used in illuminated manuscripts and are created from natural dyes by precipitating the soluble dye onto an insoluble mordant, typically a metallic salt like alum (aluminosilicates in this case) [47].



**Figure 8.** (a) RGB, (b) UVFC, and (c) IRFC images of the entire scroll. (d–f) Corresponding detail views in RGB, UVFC, and IRFC, respectively. The pink/red areas (in RGB) exhibit a strong green fluorescence in UVFC and a yellow-orange hue in IRFC, suggesting the presence of an insect-derived organic lake pigment. The blue pigment displays characteristics typical of silicate-based compounds appearing green in UVFC and showing a red-purple response in IRFC. The green areas are characterized by a dark yellow/brown appearance in UVFC and a blue hue in IRFC, strongly suggesting the use of a copper-based compound.

Moreover, Raman spectroscopy identifies vermilion or cinnabar in some pink areas related to the upper decorative motif, likely indicating its use to darken shaded regions.

The orange hue is mainly composed of lead (Pb), as shown in Figure 6. Raman spectroscopy reveals the presence of minium or red lead through the identification of the bands at  $121\text{ cm}^{-1}$  (lattice vibrations or external modes),  $150\text{ cm}^{-1}$  (lattice vibration or external mode category),  $225\text{ cm}^{-1}$  (bending modes of the Pb–O–Pb linkages or more complex lattice vibrations),  $314\text{ cm}^{-1}$  (Pb–O stretching vibrations),  $391\text{ cm}^{-1}$  (Pb–O stretching or bending modes), and  $549\text{ cm}^{-1}$  (stretching modes of the  $\text{Pb}^{\text{IV}}\text{O}_3$ ) [48], as shown in Figure 9. Minium or red lead ( $\text{Pb}_3\text{O}_4$ ) has been used as a pigment since antiquity. In the Middle Ages, it became particularly prominent in illuminated manuscripts due to its vibrant, orange-red hue, and excellent opacity, although it can undergo chromatic alterations [49].

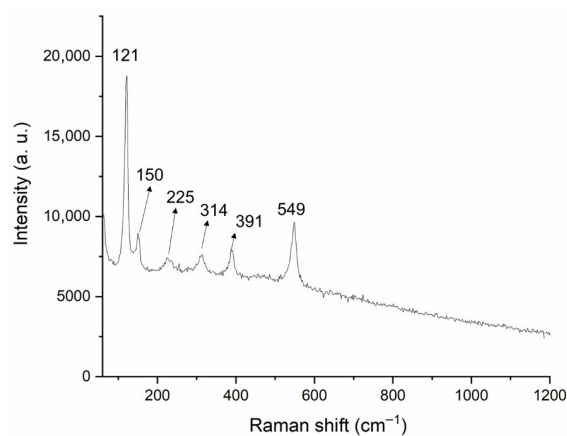


**Figure 9.** Raman spectrum of orange hue.

The blue color appears as red-purple in infrared reflectography (IRFC) and green in ultraviolet fluorescence (UVFC), as shown in Figure 8, which is typical of silicate-based

pigments [46]. MA-XRF analysis detected the presence of silicon, cobalt, and potassium (Figure 5), suggesting the use of smalt, which has the following typical composition:  $\text{SiO}_2$  (65–72%),  $\text{K}_2\text{O}$  (10–21%), and  $\text{CoO}$  (2–18%). Additionally, the presence of iron, bismuth, and arsenic can be attributed to the cobalt ore [50,51]. Infrared reflectance images further support the identification of this pigment, as at higher wavelengths (900–1700 nm), it shows significant IR absorption, appearing dark in images captured with the InGaAs camera, as illustrated in Figure 10a–c. Smalt, used as pigment by painters, shares the same qualitative chemical composition as the blue-colored glass. However, to achieve its color intensity, smalt requires a significantly higher concentration of cobalt (up to 20%) compared to the less than 2% typically found in glass. It was introduced in Europe during the 15th and 16th centuries but had been used outside of Europe as early as the 13th century [9]. In addition, the presence of As, Bi, and Fe may confirm the dating of the manuscript as being produced after 1520 [52].

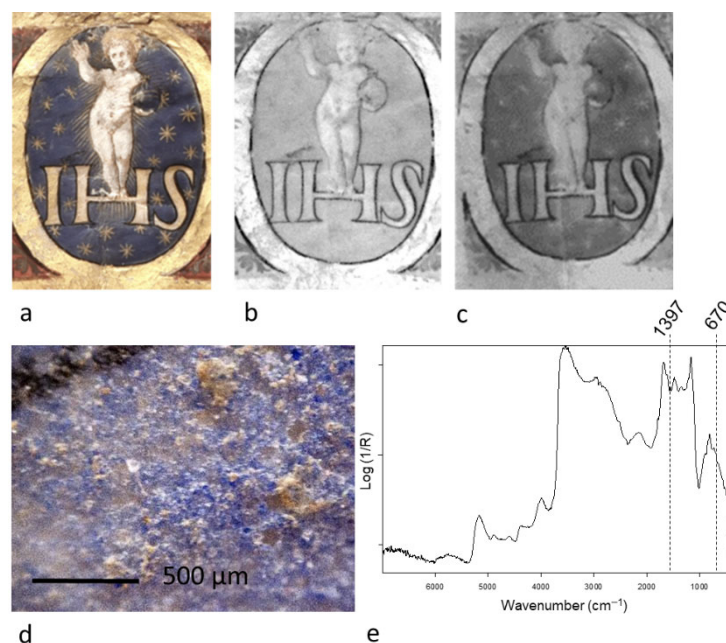


**Figure 10.** RGB image (a), IRR images of the figures taken at 1000 nm (b), and in the 900–1700 nm range (InGaAs camera) (c). Micrograph (d) and ER-FTIR spectrum (e) of the blue paint layer.

Furthermore, the XRF map shows that lead is present in all the blue pictorial layers, as illustrated in Figure 6, suggesting the use of a lead-based compound. Optical microscopy reveals the presence of white grains dispersed within the blue pictorial layer (Figure 10d), indicating that the layer is composed of multiple materials. This hypothesis is further supported by ER-FTIR analysis, which confirms the presence of lead white through its characteristic bands at  $1397^+$   $\text{cm}^{-1}$  and  $670^*$   $\text{cm}^{-1}$  (Figure 10e).

The green areas appear dark yellow/brown in the UVFC and blue in the IRFC (Figure 8), suggesting the use of copper-based compounds as confirmed by MA-XRF in Figure 6.

Raman spectroscopy, however, did not yield significant peaks attributable to the main green pigment. This lack of data is likely due to the inherent limitation of the portable instrument used, as the red laser is sub-optimal for investigating green minerals and pigments. Despite this, a localized Raman spectrum from one area (Figure 11) provided crucial secondary information. It showed peaks at 152 (w), 277 (s), 708 (w), and 1086 (vs)  $\text{cm}^{-1}$  attributed to calcium carbonate (a common filler or ground layer component). Furthermore, a distinct set of peaks (377 (s), 430 (w), 455 (w), 505 (w), 897 (w), 1116 (s), 1140 (w), 1260 (w), 1336 (w), 1377 (w), 1470 (w), 1527 (w) 1602 (w), and 2896 (vw)  $\text{cm}^{-1}$ ) could be attributed to

microcrystalline cellulose [53]. Based on the identification of this cellulose-based consolidant, we hypothesize a past restoration intervention. This assumption could be supported by the fact that cellulose is widely used in conservation treatments, and we currently lack any documentation for prior conservation work or any other known use of this compound on this type of artifact [54,55].

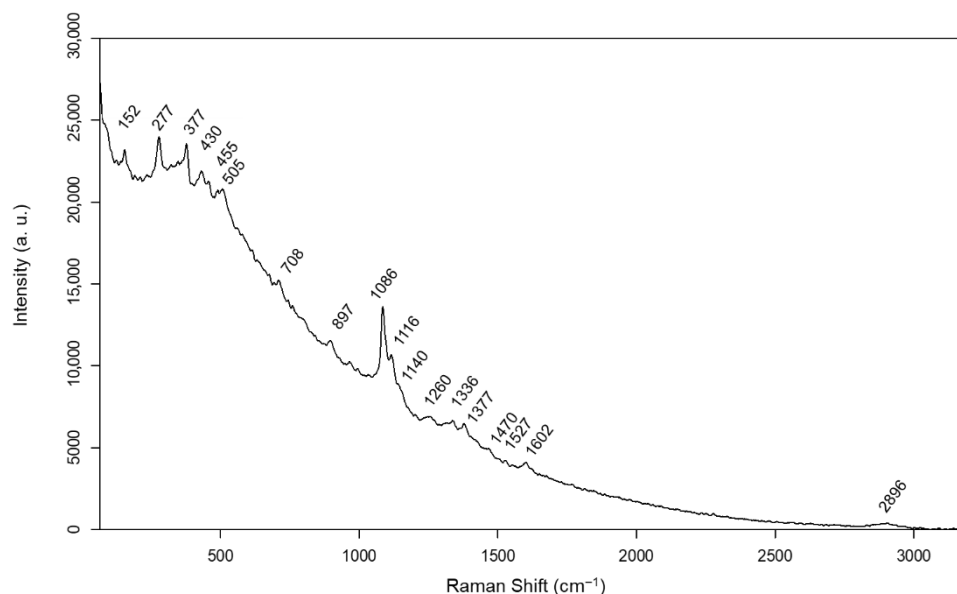


**Figure 11.** Raman spectrum acquired on the green pictorial layer containing microcrystalline cellulose.

In contrast, the green pigment was successfully identified by applying FTIR spectroscopy to several green areas. ER-FTIR spectra confirm the presence of calcite, indicated by bands at 2516, 1795, 1421<sup>+</sup>, and 876\*  $\text{cm}^{-1}$ . However, additional bands were detected at 3536\*, 2740, 2604, 2470, 2346, 2140, 2087, 2022, 1758, 1350\*, 1048\*, and 670<sup>+</sup>  $\text{cm}^{-1}$  (Figure 12). These bands could be attributed to copper hydroxynitrate  $\text{Cu}_2(\text{NO}_3)(\text{OH})_3$ , [56,57] such as rouaite or gerhardtite [58]. Particularly, the region between 2700 and 1700  $\text{cm}^{-1}$  corresponds to overtones, combination bands of the  $\text{NO}_3$  ion:  $2\nu_3$  (2740  $\text{cm}^{-1}$ ),  $\nu_1 + \nu_3$  (2470  $\text{cm}^{-1}$ ),  $\nu_3 + \nu_4$  or  $\nu_1 + \nu_3$  (2140  $\text{cm}^{-1}$ ),  $2\nu_1$  or  $\nu_3 + \nu_4$  (2087  $\text{cm}^{-1}$ ),  $2\nu_3 - \nu_4$  or  $2\nu_3 - \nu_2$ , or  $\nu_3 + \nu_4$  (2022  $\text{cm}^{-1}$ ), and  $\nu_1 + \nu_4$  (1758  $\text{cm}^{-1}$ ) [59]. The band at 2346  $\text{cm}^{-1}$  suggests the presence of trapped  $\text{CO}_2$  that could be related to the coexistence of minerals like carbonates or silicates. In fact, in addition to calcite, bands at 506<sup>+</sup> and 420<sup>+</sup>  $\text{cm}^{-1}$  are generally related to silicate-based compounds [60]. Few historical or scientific sources detail the use of this compound. As a pigment, it is quite rare, typically appearing as a replication product of historical synthetic verditer recipes. Verditer has been found in many wall and easel paintings and was initially documented in the middle of the 16th century, with production recipes recorded by the 17th century [61,62].

For the yellow hues, lead, arsenic, and calcium are detected by MA-XRF, with occasional traces of tin, particularly evident in the ovals depicting St. Thomas Aquinas and St. Peter, as well as in the yellow curtain beneath him (Figure 6). ER-FTIR analysis confirms that the calcium is associated with calcite, displaying characteristic absorption bands at 2516, 1795, 1421<sup>+</sup>, and 876\*  $\text{cm}^{-1}$ . No additional pigment contributions could otherwise be identified. Similarly, Raman spectroscopy does not reveal significant peaks, likely due to the diluted nature of the yellow hue, as observed in the microscopic image in Figure 13, especially in the one obtained through UV excitation. Furthermore, when the yellow details are more intensely colored, they are often too small to be effectively detected by the Raman and FTIR beam spot size used. Based on these analyses, we are unable to conclusively identify the pigment or pigments used for the yellow layer. However, we

can hypothesize the presence of lead-based pigments, such as lead white, massicot (PbO), and lead-tin yellow ( $\text{Pb}_2\text{SnO}_4$  or  $\text{PbSn}_{1-x}\text{Si}_x\text{O}_3$ ). Additionally, the presence of arsenic may be due to the use of orpiment (AsS) or arsenic sulfide glass, also known as artificial orpiment [63]. The period of use for orpiment, massicot, and lead-tin yellow pigments is compatible with the parchment's date [1,64]. Indeed, orpiment has a long history of use, tracing back to ancient Egypt and even prehistoric cave art [65,66]. It was a common and prized bright yellow pigment throughout the Middle Ages and the Renaissance for manuscript illuminations [67]. Despite its extreme toxicity and reactivity (often reacting with copper and lead-containing pigments, and generally not recommended for direct application on parchment), it remained in use until the 17th century [68,69]. Lead-tin yellow was extremely popular across Europe between 1300 and 1750, featuring prominently in both panel paintings and manuscript illuminations [70,71]. Finally, massicot was used as a yellow pigment from the 15th century into the early 19th century [72].

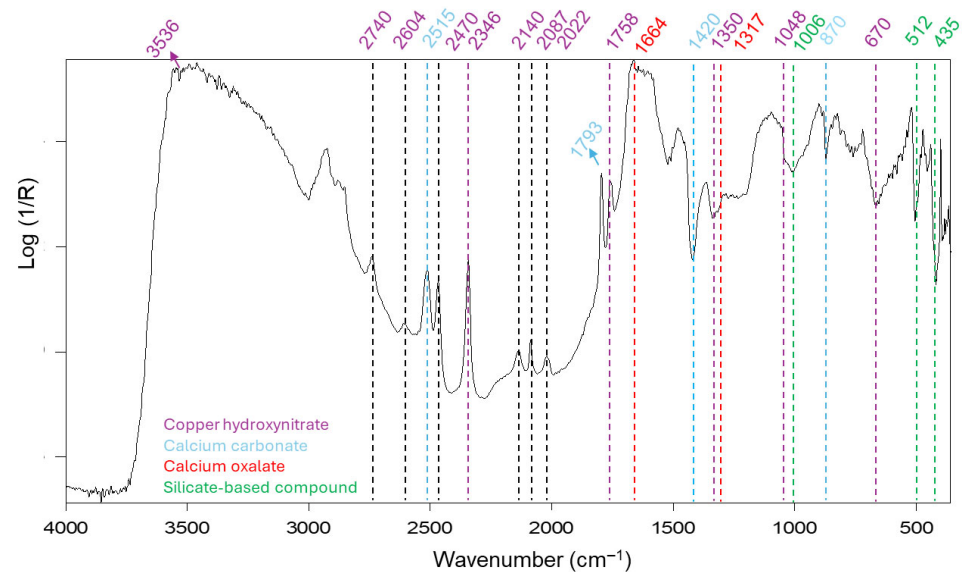


Figure 12. ER-FTIR spectrum of the green pictorial layer.

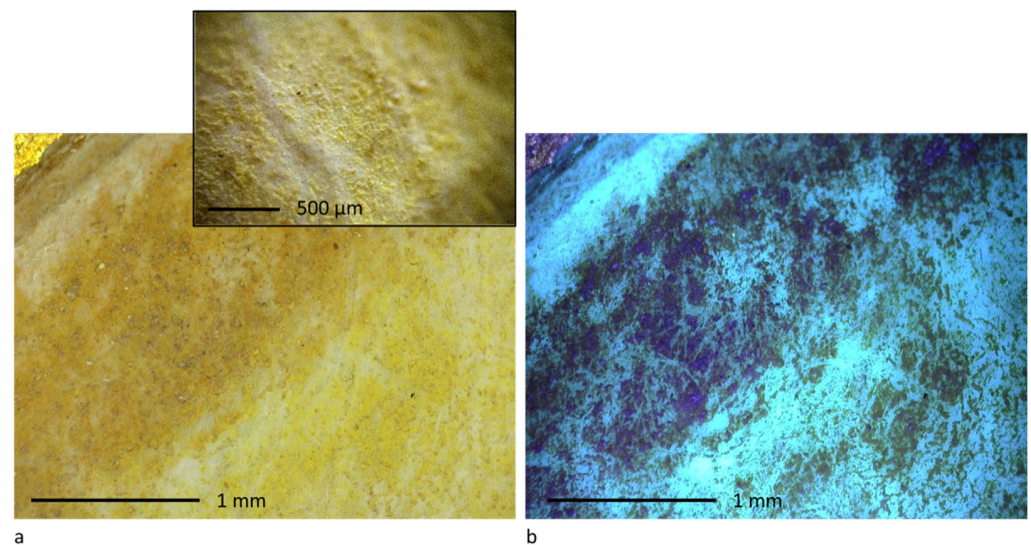
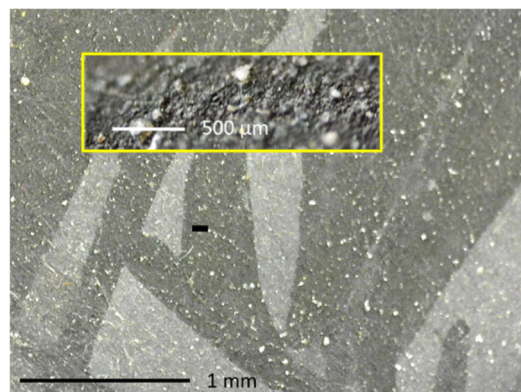


Figure 13. Micrograph image under visible (a) and UV source of a yellow painted area (b). The 20 $\times$  magnification image is reported in the image with the black contour.

Finally, IRR images reveal that black hues absorb in the infrared spectral range between 900 nm and 1700 nm (Figure 5), a behavior characteristic of carbon-based pigments.

Additionally, XRF analysis did not detect elements associated with other black pigments, such as iron or manganese. However, lead is detected within the black hues, though it cannot be definitively attributed to a specific pigment. Microscopic images, however, reveal white grains embedded in the black areas (Figure 14), suggesting a possible contribution from lead-containing materials, such as lead white.



**Figure 14.** Micrograph image of a black painted area. The 20× magnification image is reported in the yellow rectangle.

Table 1 provides a summary of the identified and hypothesized pigments.

**Table 1.** Summary of the results.

	Areas	Assignment
Preparatory layer	support additives	Parchment Calcite
Drawing	frame	Carbon-based pigment
Pictorial layer	red	Vermilion/Cinnabar
	pink	Lead white mixed with animal derivate lake (aluminosilicates as mordant)
	orange	Minium/Red lead
	blue	Smalt mixed with lead white
	green	Copper hydroxynitrate (rouaite or gerhardtite)
	yellow	Lead, arsenic, tin-based pigments
	black	Carbon-based pigment mixed with lead white
Metal layers		Gold and silver
Written text	red	Vermilion/Cinnabar and silver tip
	blue	Smalt and silver tip
	black	Iron-based ink

To summarize, the identification of lead white, vermillion/cinnabar, minium (red lead) and orpiment (hypothesis), smalt and lead-tin yellow is consistent with the dating of the scroll (1585). While lead white, vermillion/cinnabar, and minium were frequently employed across Europe from the Medieval period to the late Renaissance, smalt and lead-tin yellow were introduced the first during the 15th and 16th centuries [73] and the latter during the 13th or 14th century [70,71]. Furthermore, the identification of hydroxynitrate as a pigment within this manuscript represents a particularly intriguing and comparatively uncommon finding. Indeed, during the Renaissance, the predominant green pigments were well-documented materials such as the natural mineral malachite, or the synthetically

produced verdigris and verditer [74]. Additionally, common practice involved the preparation of greens through mixtures, such as vergaut (indigo combined with orpiment) [24]. The presence of hydroxynitrate thus warrants further examination, as it deviates from the typical green pigment repertoire of the era, potentially offering unique insights into specific workshop practices, regional variations, or experimental approaches to color formulation during the late Renaissance.

### 3.3. Metal Layers

The XRF analysis detects the use of gold (Au) for the gilding (Figure 15). Microscopical observation, shown in Figure 16(1,2), together with the shape of the MA-XRF maps (Figure 15) where the structure is visible especially in foil overlaps, suggests that metal foil is used in the circular and rectangular frames (possibly as mordant gilding for the absence of Ca and Fe), while shell gold is likely used for the small details in the figures. Silver is also detected by MA-XRF, in particular in highlights of draperies, halos, and other decorations. In this case, it is likely to be employed as shell silver (Figure 16). In the keys of Saint Peter, shown in Figure 16(3,4), it is possibly present in the form of a proper metal foil.

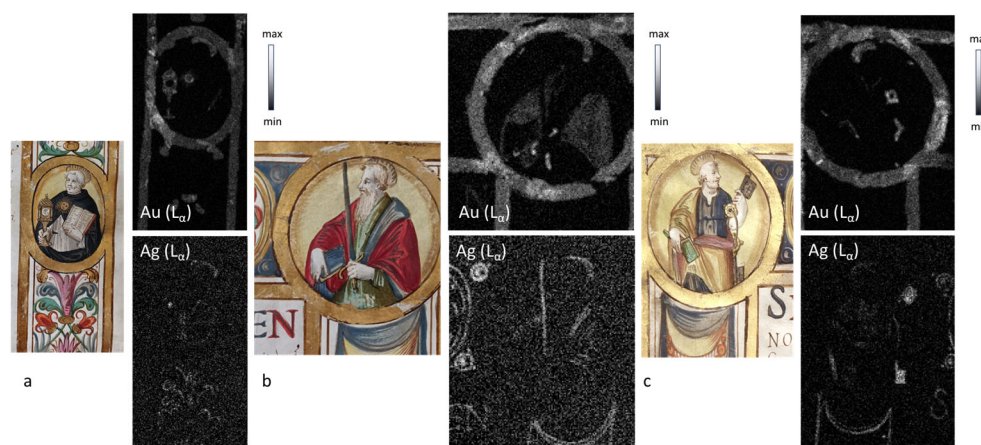


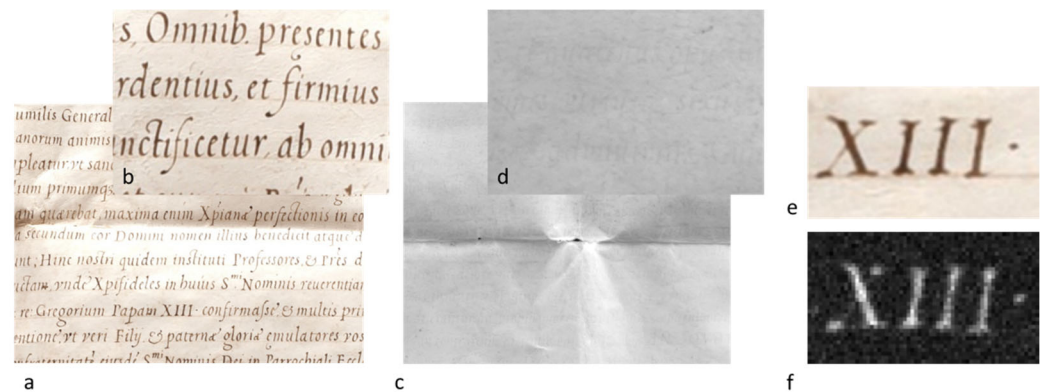
Figure 15. XRF maps of Au ( $L_{\alpha}$ ) and Ag ( $L_{\alpha}$ ) of three saints (a–c).



Figure 16. Micrographs of the gilding with two different magnifications (1,2). Micrographs of the shell silver traits on blue (3) and red (4) pictorial layers.

### 3.4. Written Text

MA-XRF analysis and IRR images confirm the use of iron-based ink for the black part of the text due to high transparency in the IRR (Figure 17) and the detection of iron.



**Figure 17.** RGB image (a) and IRR (c) images of the central section of the written part of the parchment, along with their respective magnified views (b,d). Photographic image of a detail (e) and its XRF map of Fe K $\alpha$  (f).

Moreover, UV fluorescence imaging proves particularly effective in distinguishing between the written elements and the parchment substrate. As observed in Figure 18, this technique significantly increases the contrast, enabling clearer readability of otherwise faded or difficult-to-discern letters. This heightened contrast arises from a fundamental difference in the fluorescent properties of the materials. The support, being primarily composed of collagen and calcite, exhibits a strong fluorescence emission when exposed to UV light [75,76]. In contrast, the iron-gall ink does not fluoresce under UV illumination.

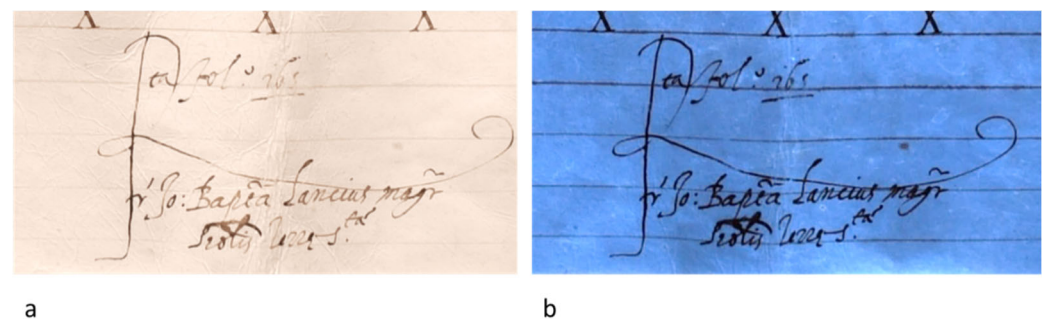


**Figure 18.** RGB image (a) and UV fluorescence image (b) of the sign.

### 3.5. Capital Letters

The capital letters are obtained with blue and red hues. For the blue hues, by observing the “chromatic similarity” image obtained from the small area in the lower part of the blue background of the central golden oval (white point in Figure 19b), it is conceivable that the same pictorial material was used for both the illustration and the capital letters (Figure 19). By observing the “chromatic similarity”, obtained from the blue hues, it becomes evident that the same pictorial layer was used for both the illustration and the capital letters (Figure 19).



**Figure 19.** RGB image (a) and chromatic similarity of the blue hues. The similarity map shown in (b) is obtained by selecting the white point in the image (a). The white pixels in (b) have high chromatic similarity; the black pixels have no similarity.

Indeed, MA-XRF maps (Figure 6) confirm that the blue pigment is characterized by cobalt potassium, iron, bismuth, and lead, as the blue pigment used for the figurative parts (Figure 6), whereas the presence of mercury (Hg) in the red pigment suggests the use of cinnabar. Moreover, shell silver is used also to highlight capital letters (Figure 20).

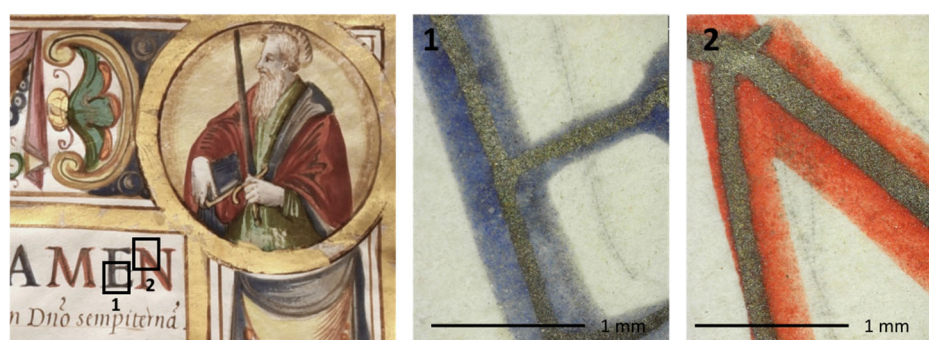


**Figure 20.** Micrographs of two capital letters “E” (1) and “N” (2) taken in the black rectangle defined in the visible image.

#### 4. Conclusions

This study highlights the importance of combining non-invasive analytical techniques to investigate and preserve illuminated manuscripts, increasing the understanding of the materials used for 16th-century parchment miniatures. Particularly, this research is the first material investigation conducted on a scroll commissioned by the Dominican Order during the Counter-Reformation in 1585 AD, which allows us to precisely document the practices of a specific workshop in Italy during this period.

By applying a multi-analytical approach, including optical microscopy, Hypercolorimetric Multispectral Imaging (HMI), infrared reflectography in the 950–1700 nm range, Fiber Optics Reflectance Spectra (FORS), macro X-ray fluorescence (MA-XRF) spectroscopy, Raman spectroscopy, and External Reflection Fourier Transform Infrared spectroscopy (ER-FTIR), significant insights were obtained into the materials and techniques employed in the creation of this artifact. The results, summarized in Table 1, indicate the use of carbon-based materials for preparatory drawings. Pure gold was confirmed for gilding, and shell silver is also detected in some highlights of both the pictures and the written text, reflecting the high value and craftsmanship of the manuscript. Mineral-based pigments such as smalt, vermilion, calcite, lead white, and copper hydroxynitrate, such as rouaite or gerhardtite, were detected. Moreover, pink hues are created with an animal-derived lake

and cinnabar in some darker areas. In contrast, the results obtained on the yellow hues suggest the presence of lead and arsenic, with occasional traces of tin, which require further investigation for precise identification. Finally, the capital letters were realized with smalt and vermilion, respectively; meanwhile, the black ink used for the text is composed of iron gall ink, a widely utilized writing material on parchment.

The multi-analytical approach employed in this study proved to be exceptionally effective for analyzing this miniature, especially considering the limitations of in situ measurements and the inability to perform analyses on micro-samples. While highly functional, certain limitations were encountered, particularly regarding the identification of pigments that were either heavily diluted intentionally or have lost material over time.

These challenges, however, can be mitigated by adopting intermediate approaches that bridge the gap between portable techniques and laboratory-based analyses. A prime example is the use of portable Raman spectroscopy coupled with a microscope. This setup offers the non-destructive advantage of in situ analysis while providing significantly enhanced spatial resolution, allowing for more precise targeting and identification of even sparsely distributed or minute pigment particles. Furthermore, although UV fluorescence imaging was utilized in the current study, UV fluorescence spectroscopy has demonstrated significant utility in other cases for the identification of organic dyes and certain inorganic pigments, which has led to important results [57].

For future research, we could expand our investigations to a broader corpus of 16th-century parchment miniatures from the same geographical region and period, integrating additional in situ techniques such as portable XRD. This would allow for a comparative study of material palettes and artistic techniques, helping to identify regional trends, specific workshops, and potentially even the practices of individual artists.

**Author Contributions:** Conceptualization, L.P.; methodology, L.P. and M.R.; formal analysis, L.P., M.R., L.L., C.C., C.P., F.B., C.R., L.C., A.M. and V.S.; investigation, L.P., M.R., L.L., C.C., C.P., C.R., L.C. and V.S.; resources, C.P., V.S., L.C., C.R. and M.C.G.; data curation, L.P., M.R., L.L., C.C., C.P., C.R., L.C., V.S. and A.M.; writing—original draft preparation, L.P.; writing—review and editing, L.P., M.R., L.L., C.C., C.P., C.R., L.C., A.M. and V.S.; supervision, M.C.G.; project administration, M.C.G.; funding acquisition, M.C.G. All authors have read and agreed to the published version of the manuscript.

**Funding:** This research was performed in part during the Training Camp “Dalla diagnostica alla fruizione museale: le opere del museo Colle del Duomo di Viterbo”, funded under the public notice of the Lazio Region Framework Agreement “Research, Technological Innovation, Thematic Networks” (APQ6)—Extract “Implementation of Programmatic Interventions and New Interventions Related to the Technological District for New Technologies Applied to Cultural Heritage and Activities.” Intervention TE1—Invitation to the Center of Excellence to submit projects for the second phase (determination 21 January 2020, no. G00471 published in BUR Lazio no. 7—Supplement no. 1 of 23 January 2020).

**Data Availability Statement:** The data supporting this study are available upon reasonable request from the corresponding author. A selection of these data is provided in the [https://drive.google.com/drive/folders/1Fd1KmRzFH8LgitMkfodc4OJXuXe-ll17?usp=drive\\_link](https://drive.google.com/drive/folders/1Fd1KmRzFH8LgitMkfodc4OJXuXe-ll17?usp=drive_link) (accessed on 18 November 2025).

**Acknowledgments:** We would like to express our sincere gratitude to the Diocese of Viterbo and the ARCHEOares Society for their hospitality and support at the monumental complex of Colle del Duomo during the Training Camp. A special thanks to Don Emanuele Germani for his kindness and willingness to allow us to further analyze the artwork at his parish, the “Parrocchia dei Santi Valentino e Ilario” in Viterbo. Moreover, we would like to thank Giacomo Viviani (INFN-LNF) for his technical support during the measurements. Finally, a special thank you to Antonella Privitera for her valuable insight into the identification of the green pigment.

**Conflicts of Interest:** The authors declare no conflicts of interest.

## References

1. Orna, M.V. Artists' pigments in illuminated medieval manuscripts: Tracing artistic influences and connections—A review. *ACS Symp. Ser.* **2013**, *1147*, 3–18. [[CrossRef](#)]
2. Panayotova, S. *The Art & Science of Illuminated Manuscripts: A Handbook*; Harvey Miller Publishers: London, UK, 2020; 528p, ISBN 9781912554591.
3. Plesters, J. 2. Ultramarine blue, natural and artificial. *Stud. Conserv.* **1966**, *11*, 62–75. [[CrossRef](#)]
4. Vetter, W.; Latini, I.; Schreiner, M. Azurite in medieval illuminated manuscripts: A reflection-FTIR study concerning the characterization of binding media. *Herit. Sci.* **2019**, *7*, 21. [[CrossRef](#)] [[PubMed](#)]
5. Cucci, C.; Delaney, J.K.; Picollo, M. Reflectance Hyperspectral Imaging for Investigation of Works of Art: Old Master Paintings and Illuminated Manuscripts. *Acc. Chem. Res.* **2016**, *49*, 2070–2079. [[CrossRef](#)] [[PubMed](#)]
6. Aceto, M.; Agostino, A.; Fenoglio, G.; Baraldi, P.; Zannini, P.; Hofmann, C.; Gamillscheg, E. First analytical evidences of precious colourants on Mediterranean illuminated manuscripts. *Spectrochim. Acta Part. A Mol. Biomol. Spectrosc.* **2012**, *95*, 235–245. [[CrossRef](#)]
7. Nodari, L.; Ricciardi, P. Non-invasive identification of paint binders in illuminated manuscripts by ER-FTIR spectroscopy: A systematic study of the influence of different pigments on the binders' characteristic spectral features. *Herit. Sci.* **2019**, *7*, 7. [[CrossRef](#)]
8. Pessanha, S.; Manso, M.; Carvalho, M.L. Application of spectroscopic techniques to the study of illuminated manuscripts: A survey. *Spectrochim. Acta Part B At. Spectrosc.* **2012**, *71–72*, 54–61. [[CrossRef](#)]
9. Ricciardi, P.; Dooley, K.A.; MacLennan, D.; Bertolotti, G.; Gabrieli, F.; Patterson, C.S.; Delaney, J.K. Use of standard analytical tools to detect small amounts of smalt in the presence of ultramarine as observed in 15th-century Venetian illuminated manuscripts. *Herit. Sci.* **2022**, *10*, 38. [[CrossRef](#)]
10. Edwards, H.G.M.; Vandenabeele, P.; Colomban, P. Analytical Raman Spectroscopy of Manuscripts and Maps: The Role of Inks. In *Raman Spectroscopy in Cultural Heritage Preservation*; Springer: Berlin/Heidelberg, Germany, 2023; pp. 215–231. [[CrossRef](#)]
11. Martinez, K.; Cupitt, J.; Saunders, D.; Pillay, R. Ten years of art imaging research. *Proc. IEEE* **2002**, *90*, 28–41. [[CrossRef](#)]
12. Del Federico, E.; Shöfberger, W.; Schelvis, J.; Kapetanaki, S.; Tyne, L.; Jerschow, A. Insight into Framework Destruction in Ultramarine Pigments. *Inorg. Chem.* **2006**, *45*, 1270–1276. [[CrossRef](#)]
13. Perino, M.; Pronti, L.; Moffa, C.; Rosellini, M.; Felici, A.C. New Frontiers in the Digital Restoration of Hidden Texts in Manuscripts: A Review of the Technical Approaches. *Heritage* **2024**, *7*, 683–696. [[CrossRef](#)]
14. Pouyet, E.; Devine, S.; Grafakos, T.; Kieckhefer, R.; Salvant, J.; Smieska, L.; Woll, A.; Katsaggelos, A.; Cossairt, O.; Walton, M. Revealing the biography of a hidden medieval manuscript using synchrotron and conventional imaging techniques. *Anal. Chim. Acta* **2017**, *982*, 20–30. [[CrossRef](#)]
15. Colantonio, C.; Clivet, L.; Laval, E.; Coquinot, Y.; Maury, C.; Melis, M.; Boust, C. Integration of multispectral imaging, XRF mapping and Raman analysis for noninvasive study of illustrated manuscripts: The case study of fifteenth century "Humay meets the Princess Humayun" Persian masterpiece from Louvre Museum. *Eur. Phys. J. Plus* **2021**, *136*, 958. [[CrossRef](#)]
16. Chiriu, D.; Ricci, P.C.; Cappellini, G. Raman characterization of XIV–XVI centuries Sardinian documents: Inks, papers and parchments. *Vib. Spectrosc.* **2017**, *92*, 70–81. [[CrossRef](#)]
17. Mercuri, F.; Buonora, P.; Cicero, C.; Helas, P.; Manzari, F.; Marinelli, M.; Paoloni, S.; Pasqualucci, A.; Pinzari, F.; Romani, M.; et al. Metastructure of illuminations by infrared thermography. *J. Cult. Herit.* **2018**, *31*, 53–62. [[CrossRef](#)]
18. Legrand, S.; Ricciardi, P.; Nodari, L.; Janssens, K. Non-invasive analysis of a 15th century illuminated manuscript fragment: Point-based vs imaging spectroscopy. *Microchem. J.* **2018**, *138*, 162–172. [[CrossRef](#)]
19. Pronti, L.; Perino, M.; Cursi, M.; Santarelli, M.L.; Felici, A.C.; Bracciale, M.P. Characterization and Digital Restoration of XIV–XV Centuries Written Parchments by Means of Nondestructive Techniques: Three Case Studies. *J. Spectrosc.* **2018**, *2018*, 1–14. [[CrossRef](#)]
20. Titubante, M.; Giannini, F.; Pasqualucci, A.; Romani, M.; Verona-Rinati, G.; Mazzuca, C.; Micheli, L. Towards a non-invasive approach for the characterization of Arabic/Christian manuscripts. *Microchem. J.* **2020**, *155*, 104684. [[CrossRef](#)]
21. Turner, N.K.; Patterson, C.S.; MacLennan, D.K.; Trentelman, K. Visualizing underdrawings in medieval manuscript illuminations with macro-X-ray fluorescence scanning. *X-Ray Spectrom.* **2019**, *48*, 251–261. [[CrossRef](#)]
22. Deneckere, A.; De Reu, M.; Martens, M.P.J.; De Coene, K.; Vekemans, B.; Vincze, L.; De Maeyer, P.; Vandenabeele, P.; Moens, L. The use of a multi-method approach to identify the pigments in the 12th century manuscript Liber Floridus. *Spectrochim. Acta Part A Mol. Biomol. Spectrosc.* **2011**, *80*, 125–132. [[CrossRef](#)]
23. Tonazzini, A.; Salerno, E.; Abdel-Salam, Z.A.; Harith, M.A.; Marras, L.; Botto, A.; Campanella, B.; Legnaioli, S.; Pagnotta, S.; Poggialini, F.; et al. Analytical and mathematical methods for revealing hidden details in ancient manuscripts and paintings: A review. *J. Adv. Res.* **2019**, *17*, 31–42. [[CrossRef](#)]
24. Perino, M.; Pronti, L.; Di Forti, L.G.; Romani, M.; Taverna, C.; Massolo, L.; Manzari, F.; Cestelli-Guidi, M.; Nucara, A.; Felici, A.C. Revealing artists' collaboration in a 14th century manuscript by non-invasive analyses. *Minerals* **2021**, *11*, 771. [[CrossRef](#)]

25. Mounier, A.; Le Bourdon, G.; Aupetit, C.; Belin, C.; Servant, L.; Lazare, S.; Lefrais, Y.; Daniel, F. Hyperspectral imaging, spectrofluorimetry, FORS and XRF for the non-invasive study of medieval miniatures materials. *Herit. Sci.* **2014**, *2*, 24. [CrossRef]
26. Nastova, I.; Grupče, O.; Minčeva-Šukarova, B.; Ozcatal, M.; Mojsoska, L. Spectroscopic analysis of pigments and inks in manuscripts: I. Byzantine and post-Byzantine manuscripts (10–18th century). *Vib. Spectrosc.* **2013**, *68*, 11–19. [CrossRef]
27. Mazzinghi, A.; Ruberto, C.; Castelli, L.; Ricciardi, P.; Czelusniak, C.; Giuntini, L.; Mandò, P.A.; Manetti, M.; Palla, L.; Taccetti, F. The importance of being little: MA-XRF on manuscripts on a Venetian island. *X-Ray Spectrom.* **2021**, *50*, 272–278. [CrossRef]
28. Marucci, G.; Beeby, A.; Parker, A.W.; Nicholson, C.E. Raman spectroscopic library of medieval pigments collected with five different wavelengths for investigation of illuminated manuscripts. *Anal. Methods* **2018**, *10*, 1219–1236. [CrossRef]
29. Mash'al, N.; Razak, R.A.; Sharif, H.M. A review on methods of analysis of the pigments and inks in illuminated manuscript. *J. Archit. Plan. Constr. Manag.* **2023**, *13*, 77–89.
30. Tanevska, V.; Nastova, I.; Minčeva-Šukarova, B.; Grupče, O.; Ozcatal, M.; Kavčić, M.; Jakovlevska-Spirovska, Z. Spectroscopic analysis of pigments and inks in manuscripts: II. Islamic illuminated manuscripts (16th–18th century). *Vib. Spectrosc.* **2014**, *73*, 127–137. [CrossRef]
31. Faubel, W.; Staub, S.; Simon, R.; Heissler, S.; Pataki, A.; Banik, G. Non-destructive analysis for the investigation of decomposition phenomena of historical manuscripts and prints. *Spectrochim. Acta Part B At. Spectrosc.* **2007**, *62*, 669–676. [CrossRef]
32. Melis, M.; Miccoli, M.; Quarta, D. Multispectral hypercolorimetry and automatic guided pigment identification: Some masterpieces case studies. *Opt. Metrol.* **2013**, *8790*, 87900W. [CrossRef]
33. Melis, M.; Miccoli, M. Trasformazione evolutivistica di una fotocamera reflex digitale in un sofisticato strumento per misure fotometriche e colorimetriche. In *Colore e Colorimetria Contributi Multidisciplinari*; Maggioli Editore: Santarcangelo di Romagna, Italy, 2013; pp. 28–38.
34. Laureti, S.; Colantonio, C.; Burrascano, P.; Melis, M.; Calabrò, G.; Malekmohammadi, H.; Sfarra, S.; Ricci, M.; Pelosi, C. Development of integrated innovative techniques for paintings examination: The case studies of The Resurrection of Christ attributed to Andrea Mantegna and the Crucifixion of Viterbo attributed to Michelangelo's workshop. *J. Cult. Herit.* **2019**, *40*, 1–16. [CrossRef]
35. Annarilli, S.; Casoli, A.; Colantonio, C.; Lanteri, L.; Marseglia, A.; Pelosi, C.; Sottile, S. A Multi-Instrument Analysis of the Late 16th Canvas Painting, "Coronation of the Virgin with the Saints Ambrose and Jerome", Attributed to the Tuscany-Umbria Area to Support the Possibility of Bio-Cleaning Using a Bacteria-Based System. *Heritage* **2022**, *5*, 2904–2921. [CrossRef]
36. Bonizzoni, L.; Caglio, S.; Galli, A.; Lanteri, L.; Pelosi, C. Materials and Technique: The First Look at Saturnino Gatti. *Appl. Sci.* **2023**, *13*, 6842. [CrossRef]
37. Taccetti, F.; Castelli, L.; Czelusniak, C.; Gelli, N.; Mazzinghi, A.; Palla, L.; Ruberto, C.; Censori, C.; Lo Giudice, A.; Re, A.; et al. A multipurpose X-ray fluorescence scanner developed for in situ analysis. *Rend. Lincei* **2019**, *30*, 307–322. [CrossRef]
38. Rosi, F.; Cartechini, L.; Sali, D.; Miliani, C. Recent trends in the application of Fourier Transform Infrared (FT-IR) spectroscopy in Heritage Science: From micro- to non-invasive FT-IR. *Phys. Sci. Rev.* **2019**, *4*, 20180006. [CrossRef]
39. Miliani, C.; Rosi, F.; Daveri, A.; Brunetti, B.G. Reflection infrared spectroscopy for the non-invasive in situ study of artists' pigments. *Appl. Phys. A Mater. Sci. Process.* **2012**, *106*, 295–307. [CrossRef]
40. Botticelli, M.; Maras, A.; Candeias, A.  $\mu$ -Raman as a fundamental tool in the origin of natural or synthetic cinnabar: Preliminary data. *J. Raman Spectrosc.* **2020**, *51*, 1470–1479. [CrossRef]
41. Nöller, R. Cinnabar reviewed: Characterization of the red pigment and its reactions. *Stud. Conserv.* **2015**, *60*, 79–87. [CrossRef]
42. Arinto, A.A.F.L.G. Chapter 9: X-ray Fluorescence Spectrometry as a diagnostic tool in conservation of illuminated manuscripts. In *Cultural Heritage: Protection, Developments and International Perspectives*; Nova Science Publishers: New York, NY, USA, 2013; pp. 235–256.
43. Mozgawa, W.; Handke, M.; Jastrzebski, W. Vibrational spectra of aluminosilicate structural clusters. *J. Mol. Struct.* **2004**, *704*, 247–257. [CrossRef]
44. Bisulca, C.; Piccolo, M.; Bacci, M.; Kunzelman, D. Uv-Vis-Nir Reflectance Spectroscopy of Red Lakes in Paintings. In Proceedings of the 9th International Conference on NDT of Art (Nondestructive Testing of Art), Jerusalem, Israel, 25–30 May 2008; pp. 1–7.
45. Cosentino, A. Effects of Different Binders on Technical Photography and Infrared Reflectography of 54 Historical Pigments. *Int. J. Conserv. Sci.* **2015**, *6*, 287–298.
46. Boust, C.; Wohlgelmuth, A. DATABASE: Pigments under UV and IR radiations. *Sci. Imaging Cult. Herit.* **2017**. Available online: <https://copa.hypotheses.org/552> (accessed on 18 November 2025).
47. Melo, M.J.; Nabais, P.; Guimarães, M.; Araújo, R.; Castro, R.; Oliveira, M.C.; Whitworth, I. Organic dyes in illuminated manuscripts: A unique cultural and historic record. *Philos. Trans. R. Soc. A Math. Phys. Eng. Sci.* **2016**, *374*, 20160050. [CrossRef] [PubMed]
48. Amat, A.; Rosi, F.; Miliani, C.; Sassi, P.; Paolantoni, M.; Fantacci, S. A combined theoretical and experimental investigation of the electronic and vibrational properties of red lead pigment. *J. Cult. Herit.* **2020**, *46*, 374–381. [CrossRef]

49. Aze, S.; Vallet, J.-M.; Detalle, V.; Grauby, O.; Baronnet, A. Chromatic alterations of red lead pigments in artworks: A review. *Phase Transit.* **2008**, *81*, 145–154. [[CrossRef](#)]
50. Dehaine, Q.; Tijsseling, L.T.; Glass, H.J.; Törmänen, T.; Butcher, A.R. Geometallurgy of cobalt ores: A review. *Miner. Eng.* **2021**, *160*, 106656. [[CrossRef](#)]
51. Nimis, P.; Costa, L.D.; Guastoni, A. Cobaltite-rich mineralization in the iron skarn deposit of Traversella (Western Alps, Italy). *Mineral. Mag.* **2014**, *78*, 11–27. [[CrossRef](#)]
52. Cavallo, G.; Riccardi, M.P. Glass-based pigments in painting: Smalt blue and lead–tin yellow type II. *Archaeol. Anthropol. Sci.* **2021**, *13*, 199. [[CrossRef](#)]
53. Agarwal, U.P. Analysis of Cellulose and Lignocellulose Materials by Raman Spectroscopy: A Review of the Current Status. *Molecules* **2019**, *24*, 1659. [[CrossRef](#)]
54. Abdel-Hamied, M.; Abdelhafez, A.A.M.; Abdel-Maksoud, G. Consolidation materials used with illuminated and non-illuminated paper manuscripts and historical leather bindings: A review. *Pigment. Resin. Technol.* **2025**, *54*, 333–342. [[CrossRef](#)]
55. Beöthy-Kozocsa, I.; Sipos-Richter, T.; Szlabey, G. Parchment Codex Restoration Using Parchment and Cellulose Fibre Pulp. *Restaurator* **1990**, *11*, 95–109. [[CrossRef](#)]
56. Henrist, C.; Traina, K.; Hubert, C.; Toussaint, G.; Rulmont, A.; Cloots, R. Study of the morphology of copper hydroxynitrate nanoplatelets obtained by controlled double jet precipitation and urea hydrolysis. *J. Cryst. Growth* **2003**, *254*, 176–187. [[CrossRef](#)]
57. Zhan, Y.; Zhou, X.; Fu, B.; Chen, Y. Catalytic wet peroxide oxidation of azo dye (Direct Blue 15) using solvothermally synthesized copper hydroxide nitrate as catalyst. *J. Hazard. Mater.* **2011**, *187*, 348–354. [[CrossRef](#)]
58. Bushong, E.J.; Yoder, C.H. The Synthesis and Characterization of Rouaite, a Copper Hydroxy Nitrate. An Integrated First-Year Laboratory Project. *J. Chem. Educ.* **2009**, *86*, 80–81. [[CrossRef](#)]
59. Secco, E.A.; Wort, G.G. Infrared spectra of unannealed and of annealed  $\text{Cu}_4(\text{OH})_6(\text{NO}_3)_2$ . *Can. J. Chem.* **1987**, *65*, 2504–2508. [[CrossRef](#)]
60. Fanost, A.; Gimat, A.; de Viguerie, L.; Martinetto, P.; Giot, A.C.; Clémancey, M.; Blondin, G.; Gaslain, F.; Glanville, H.; Walter, P.; et al. Revisiting the identification of commercial and historical green earth pigments. *Colloids Surf. A Physicochem. Eng. Asp.* **2020**, *584*, 124035. [[CrossRef](#)]
61. Purdy, E.H.; Critchley, S.; Holé, C.; Cotte, M.; Kirkham, A.; Casford, M. Characterisation of rouaite, an unusual copper-containing pigment in early modern English wall paintings, by synchrotron micro X-Ray diffraction and micro X-Ray absorption spectroscopy. *Appl. Phys. A* **2024**, *130*, 817. [[CrossRef](#)]
62. Purdy, E.H.; Critchley, S.; Kirkham, A.; Casford, M. Illuminating the problem of blue verditer synthesis in the early modern English period: Chemical characterisation and mechanistic understanding. *npj Herit. Sci.* **2024**, *12*, 138. [[CrossRef](#)]
63. Burgio, L.; Manca, R.; Browne, C.; Button, V.; Horsfall Turner, O.; Rutherford, J. Orange for gold? Arsenic sulfide glass on the V&A Lemna Album. *J. Raman Spectrosc.* **2019**, *50*, 1169–1176. [[CrossRef](#)]
64. Agresti, G.; Baraldi, P.; Pelosi, C.; Santamaria, U. Yellow pigments based on lead, tin, and antimony: Ancient recipes, synthesis, characterization, and hue choice in artworks. *Color. Res. Appl.* **2016**, *41*, 226–231. [[CrossRef](#)]
65. Brøns, C.; Thavapalan, S.; Dardeniz, G.; Hodgkinson, A.K.; Moutsiou, T.; Blakolmer, F.; Pelletier-Michaud, L. *The Value of Colour. Material and Economic Aspects in the Ancient World*; Edition Topoi: Berlin, Germany, 2019. [[CrossRef](#)]
66. Schafer, E.H. Orpiment and Realgar in Chinese Technology and Tradition. *J. Am. Orient. Soc.* **1955**, *75*, 73. [[CrossRef](#)]
67. Edwards, H.G.M. Analytical Raman spectroscopic discrimination between yellow pigments of the Renaissance. *Spectrochim. Acta Part A Mol. Biomol. Spectrosc.* **2011**, *80*, 14–20. [[CrossRef](#)]
68. van Loon, A.; Noble, P.; Krekeler, A.; Snickt, G.; Janssens, K.; Abe, Y.; Nakai, I.; Dik, J. Artificial orpiment, a new pigment in Rembrandt's palette. *Herit. Sci.* **2017**, *5*, 1. [[CrossRef](#)]
69. Muralha, V.S.F.; Burgio, L.; Clark, R.J.H. Raman spectroscopy analysis of pigments on 16–17th c. Persian manuscripts. *Spectrochim. Acta Part A Mol. Biomol. Spectrosc.* **2012**, *92*, 21–28. [[CrossRef](#)] [[PubMed](#)]
70. Kühn, H. 4 lead-tin yellow. *Stud. Conserv.* **1968**, *13*, 7–33. [[CrossRef](#)]
71. Sandalinas, C.; Ruiz-Moreno, S. Lead-tin-antimony yellow: Historical manufacture, molecular characterization and identification in seventeenth-century Italian painting. *Stud. Conserv.* **2004**, *49*, 41–52. [[CrossRef](#)]
72. Bevilacqua, N.; Borgioli, L.; Adrover Garcia, I.I. *Pigmenti nell'Arte dalla Preistoria alla Rivoluzione Industriale*; Il Prato: Villatora, Italy, 2010; ISBN 8863360901.
73. Mühlethaler, B.; Thissen, J. Smalt. *Stud. Conserv.* **1969**, *14*, 47–61. [[CrossRef](#)]
74. Riccardi, P.; Pallipurath, A.; Rose, K. "It's not easy being green": A spectroscopic study of green pigments used in illuminated manuscripts. *Anal. Methods* **2013**, *5*, 3819–3824. [[CrossRef](#)]

75. Toffolo, M.B.; Ricci, G.; Caneve, L.; Kaplan-Ashiri, I. Luminescence reveals variations in local structural order of calcium carbonate polymorphs formed by different mechanisms. *Sci. Rep.* **2019**, *9*, 16170. [[CrossRef](#)] [[PubMed](#)]
76. Dolgin, B.; Bulatov, V.; Schechter, I. A complex analytical method for parchment characterization. *Rev. Anal. Chem.* **2009**, *28*, 151–307. [[CrossRef](#)]

**Disclaimer/Publisher’s Note:** The statements, opinions and data contained in all publications are solely those of the individual author(s) and contributor(s) and not of MDPI and/or the editor(s). MDPI and/or the editor(s) disclaim responsibility for any injury to people or property resulting from any ideas, methods, instructions or products referred to in the content.